Experimental and Theoretical Research on Cogging Torque of PM Synchronous Motors Considering Manufacturing Tolerances

Jing Ou, *Student Member, IEEE*, Yingzhen Liu, *Student Member, IEEE*, Ronghai Qu, *Senior Member, IEEE*, and Martin Doppelbauer

***Abstract*—This paper investigates the cogging torque caused by manufacturing tolerances through analytical, finite element analysis (FEA), and experimental methods. Based on experiments, it is found that the stator and rotor tolerances of PM motor generate low-frequency components of cogging torque, such as the multiples of rotor pole and stator slot numbers. First, analytical calculation is used to find out the frequency spectrum components of the cogging torque. Then, FEA is used to confirm the analytical results and to determine which tolerances play dominant role on causing these components. Furthermore, the sensitivities of the key tolerances are illustrated. These can provide the designer a direction to design a motor with low sensitivity to tolerances. Because the tolerances of stator and rotor stacks are from stamping die, these tolerances are almost constant. A simple manufacturing method, i.e., rotation lamination, is proposed to manufacture the improved stator and rotor stacks. After using the proposed method, the effects of stator and rotor tolerances are individually validated through experiments.**

***Index Terms*—Cogging torque, manufacturing tolerances, rotation lamination, rotor tolerances, servo motor, surface-mounted permanent magnet synchronous motor (SPMSM), stator tolerances.**

I. Introduction

PERMANENT magnet (PM) motors have been widely used in a variety of applications due to their high torque densities, power factors, and efficiencies [1], [2]. In order to obtain a compact structure, a slotted stator is commonly used. This design inherently generates cogging torque. The rotor has the tendency to align with the slotted stator in a number of stable positions. In some applications such as steering, precision tooling, and robotics, cogging torque may affect the control accuracy and cause intolerable vibrations and acoustic noise [3]–[6]. It also limits the performance of the machine in tracking applications [7].

To reduce the cogging torque, many methods have been proposed, such as stator slot skewing (stator teeth can be straight), skewed rotor pole, closed slot, unequal pole width [8], auxiliary slots [9], and slot-opening shifting [10]. It is well known that the cogging torque frequencies are equivalent to a multiple of the least common multiple (LCM) of the rotor pole and stator slot referred to as, fundamental components. Actually because of manufacturing tolerances, motors also consist of low-frequency high-amplitude cogging torque components, which are multiples of the pole and slot numbers, respectively.

In the previous investigations, more attention was paid to the rotor eccentricities [11]–[16]. Nevertheless, according to Kim *et al.* [15], rotor eccentricities are not the main factors. Since experimental verification is challenging and finite element analysis (FEA) is time-consuming, in [3], mathematical method is used for predicting effects of manufacturing variation. In [15] and [17], the cogging torque components caused by nonuniform air gap, slot opening change, phase modulation (PM) remanence and position tolerances, and rotor eccentricity of PM machines having modular stators are analyzed. In [18], the nonuniform magnetic performance of PMs and stator out-of-roundness in interior PM machines were analyzed. In [16] and [19], the PM tolerances on dimensions, position, and magnetization direction were investigated. In order to conduct a systematical and comprehensive investigation on the effects of manufacturing tolerances, and give a clear answer through analytical, FEA and experimental methods, in this paper, the effects of all the possible tolerances are comprehensively investigated. The key factors, which play dominant role on causing low frequency cogging torque components, are determined. Furthermore, the sensitivities of key tolerances are analyzed. These can provide the designer a direction to design a motor with low sensitivity to tolerances. To reduce, separate, and experimentally verify the effects of stator and rotor tolerances, a rotation lamination method is proposed. Then, the influences of stator and rotor tolerances are individually validated through experiments. By comparing the tested results of original and improved prototypes, the validity of the analyses on this paper are proved.

Manuscript received May 18, 2017; revised July 26, 2017; accepted September 16, 2017. Date of publication October 2, 2017; date of current version January 16, 2018. *(Corresponding author: Yingzhen Liu.)*

J. Ou and M. Doppelbauer are with the Institute of Electrical Engineering, Karlsruhe Institute of Technology, Karlsruhe 76131, Germany (e-mail: jing.ou@kit.edu; martin.doppelbauer@kit.edu).

Y. Liu is with the Institute of Technical Physics, Karlsruhe Institute of Technology, Karlsruhe 76344, Germany (e-mail: yingzhen.liu@kit.edu).

R. Qu is with the State Key Laboratory of Advanced Electromagnetic Engineering and Technology, School of Electrical and Electronic Engineering, Huazhong University of Science and Technology, Wuhan 430074, China (e-mail: ronghaiqu@hust.edu.cn).

Color versions of one or more of the figures in this paper are available online at http://ieeexplore.ieee.org.

Digital Object Identifier 10.1109/TIE.2017.2758760

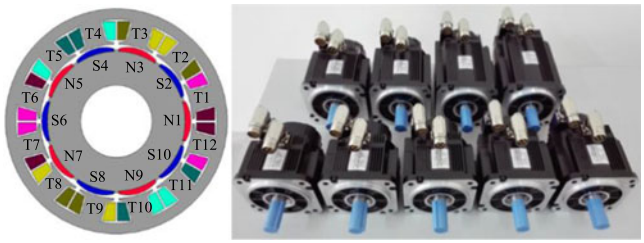

Fig. 1. Structure and prototypes of the analyzed motors.

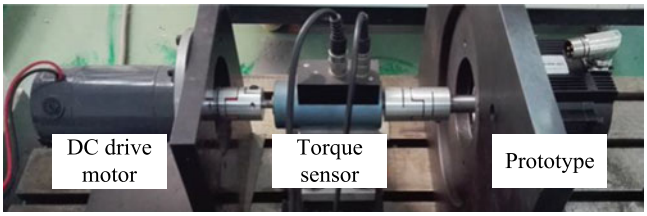

Fig. 2. Test bench.

In this paper, a 10-pole/12-slot fractional-slot surface-mounted PM synchronous motor (SPMSM) is analyzed as an example. The research results are also applicative for other poles/slots combinations. The structure and a series of prototypes of the analyzed SPMSM are shown in Fig. 1. In Fig. 1, N1–N9 and S2–S10 represent and show the positions of the ten PM poles on a rotor. T1–T12 show the positions of the 12 teeth.

This paper is structured as follows: first, the cogging torque experiment results of the original prototypes with original rotors and stators, which have skewed and unskewed stators or stators with different stack lengths are measured, presented, and discussed in Section II. Next, through analytical analysis, the cogging torque components in ideal case and caused by stator and rotor tolerances are calculated, and the relationship between tolerances and cogging torque components are determined in Section III. In Section IV, the tolerance level of the prototypes is assessed. With the help of FEA, the analytical results are verified; the importance of tolerances is discussed; and the sensitivities of key tolerances are illustrated. Then, in Section V, to separate and eliminate the influence of the tolerances of rotor and stator stacks, rotation lamination method is proposed to build the improved stator and rotor stacks. An even-PM rotor is selected for experiment verification of the stator tolerance. The experimental results successfully verify the analytical and FEA results. Finally, the conclusion is drawn in Section VI.

II. Cogging Torque From Experiments

A series of prototypes with the same stators but different stack lengths for different rated-torque levels are built and tested. In order to avoid the influence from the drive motor, a low-speed (2 r/min) dc planet gear motor is used. The rated torque and the reduction ratio of the dc motor are 500 mN·m and 1370, respectively. The measuring range of torque sensor is 0–500 mN·m and its measuring error is smaller than ±0.2%. The sampling rate is 1000 times per second. The test bench is shown in Fig. 2.

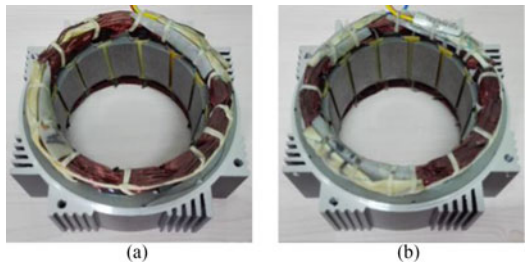

Fig. 3. Stators of the prototypes. (a) Skewed (6°). (b) Unskewed.

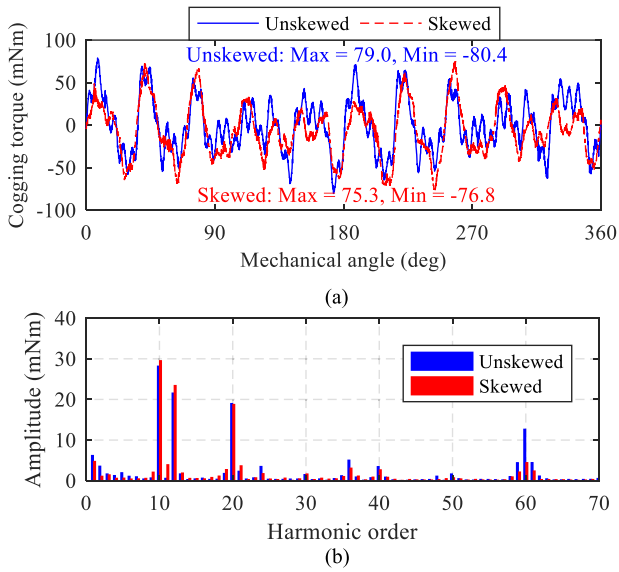

Fig. 4. Experimental results of original prototypes with unskewed and skewed stators.

The unskewed and the skewed stators of the prototypes, whose stack lengths are 38 mm and rated-torque is 5.4 N·m are shown in Fig. 3. The experimental results of the two prototypes are compared and illustrated in Fig. 4. By employing the slot skewing method, the fundamental cogging torque component (amplitude of the 60th order) is dramatically decreased as shown in Fig. 4(b). However, the peak-to-peak value of cogging torque is hardly reduced as the low-frequency components have high amplitudes (especially the 10th, 12th, and 20th). These low-frequency components are referred as additional cogging torque components in this paper.

To exclude individual phenomena, four more prototypes with larger stack lengths (66 mm), named P1, P2, P3, and P4, whose rated-torque is 9.6 N·m, are also tested and the test results are shown in Fig. 5. The same components with diverse amplitudes were obtained. Fig. 5(b) clearly shows that the cogging torque components of some of the prototypes have very low amplitudes of the 12th order, but the amplitudes of the 10th and 20th orders are always very high.

It is well known that, these components are caused by manufacturing tolerances. To ascertain the relationship between tolerance and cogging torque components and the importance of tolerances, analytical, FEA, and experimental methods will be used in the following sections.

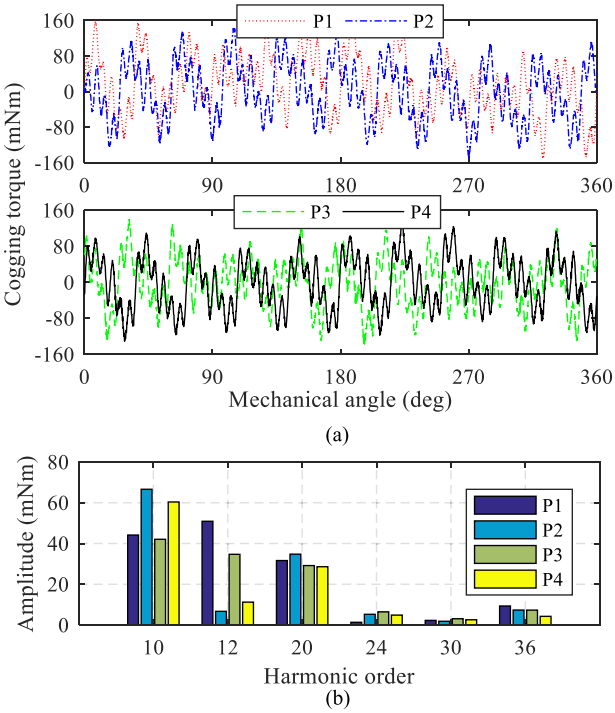

Fig. 5. Experimental results of four original prototypes with larger stack lengths.

III. Theoretical Analysis

Several methods to predict the cogging torque in SPMSM, such as energy variation [20], Maxwell stress tensor [21], [22], and FEA, are already available. The energy variation method can be used to quickly predict the frequency of the cogging torque and determine the skewing angle of rotor pole or stator slot. However, this method exhibits a large error in amplitude and waveform of the cogging torque [23], [24]. By using the Maxwell stress tensor method to calculate the cogging torque of each slot, the cogging torque waveform and amplitude have a high precision. However, the relationship between the tolerance and the frequency of cogging torque in the equation is not obvious. The FEA method also has high precision in amplitude and waveform. However, it is not only time-consuming but also does not clearly show the relationship between the frequency of cogging torque and the tolerance. Hence, in order to quickly determine the relationship between each tolerance and specific order of the cogging torque components, energy variation is used since its variation frequencies are directly reflect to the latter. By means of FEA, the importance of each tolerance is compared.

A. Cogging Torque for Ideal Case

Based on the energy method, cogging torque $T_{\rm cog}$ can be expressed as

$$T_{\rm cog}(\alpha) = -\frac{\partial W(\alpha)}{\partial \alpha} \tag{1}$$

where α is the position angle of the stator when the rotor is considered as static and the stator rotates.

By neglecting the fringing and considering the permeability of iron steel to be infinite, the energy W on the air gap and magnets can be calculated as

$$W(\alpha) = \frac{1}{2\mu_0}\int_V B_r^2(\theta)\left(\frac{h_m}{h_m + g(\theta,\alpha)}\right)^2 dV \tag{2}$$

where B_r is the remanence of PM, h_m is the thickness of PM in magnetization direction, g is the length of physical air gap, and θ is the angle along the circumference.

Substituting (2) to (1), one can express the cogging torque as follows [16]:

$$T_{\rm cog}(\alpha) = -\frac{L_{\rm Fe}}{4\mu_0}\left(R_2^2 - R_1^2\right)\frac{\partial}{\partial\alpha}\int_0^{2\pi} F^2(\theta)\Lambda^2(\theta,\alpha)d\theta \tag{3}$$

where $L_{\rm Fe}$ is the effective axial length of the motor; R_2 and R_1 are the outer and inner radii of the air gap, respectively; $F(\theta)$ is the air gap magnetic potential; and $\Lambda(\theta,\ \alpha)$ is the air gap relative permeance in an equivalent slotless machine.

$F^2(\theta)$ and $\Lambda^2\ (\theta,\ \alpha)$ can be expressed as follows:

$$F^2(\theta) = B_r^2(\theta)h_m^2, \quad \Lambda^2(\theta,\alpha) = \left(\frac{1}{h_m + g(\theta,\alpha)}\right)^2. \tag{4}$$

If the pole number is $2p$ and the slot number is z, the Fourier series of (4) can be rewritten as (5) and (6), respectively, shown below, and the coefficients of each term can be expressed as (7) and (8)

$$F^2(\theta) = F_0 + \sum_{n=1}^{\infty} F_n\cos(2pn\theta) \tag{5}$$

$$\Lambda^2(\theta,\alpha) = \Lambda_0 + \sum_{n=1}^{\infty}\Lambda_n\cos\left(nz\left(\alpha+\theta\right)\right) \tag{6}$$

$$F_0 = B_r^2h_m^2\alpha_p, \quad F_n = \frac{2F_0}{n\pi\alpha_p}\sin\left(n\pi\alpha_p\right) \tag{7}$$

$$\Lambda_0 = \left(\frac{1}{h_m+g}\right)^2\alpha_\tau, \quad \Lambda_n = \frac{2\Lambda_0}{n\pi\alpha_\tau}\sin\left(n\pi\alpha_\tau\right) \tag{8}$$

where α_p is the ratio of pole width w_p to pole pitch τ_p, and α_τ is the ratio of tooth-shoe width w_τ to slot pitch τ_s.

By substituting (5) and (6) to (3), the cogging torque can be rewritten as follows:

$$\begin{aligned} T_{\rm cog}(\alpha) &= -\frac{L_{\rm Fe}}{4\mu_0}\left(R_2^2 - R_1^2\right)\frac{\partial}{\partial\alpha}\int_0^{2\pi}\sum_{n=1}^{\infty}F_n\cos(2pn\theta) \\ &\quad\cdot\sum_{n=1}^{\infty}\Lambda_n\cos\left(nz\left(\alpha+\theta\right)\right)d\theta \\ &= \frac{\pi L_{\rm Fe}}{4\mu_0}\left(R_2^2 - R_1^2\right)\sum_{n=1}^{\infty}nLF_{n\frac{L}{2p}}\Lambda_{n\frac{L}{z}}\sin(nL\alpha) \end{aligned} \tag{9}$$

where L is LCM of the rotor pole and stator slot.

From (9), it can be known that the cogging torque consists of a series of components whose frequencies are equivalent to a multiple of LCM. If the slot skewing method is used to reduce cogging torque, the skewing angle is equal to $360/L$; if two segments of a skewed rotor pole are used, the skewing angle is equal to $180/L$.

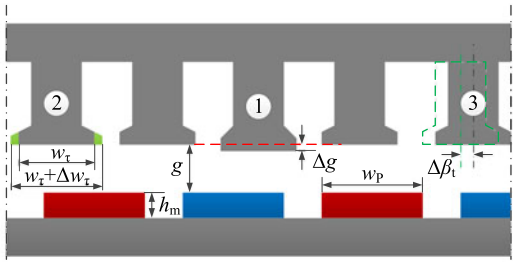

Fig. 6. Manufacturing tolerances on the stator.

For the prototypes with 10-poles/12-slots, L is equal to 60. Thus, the 60th harmonic is the cogging torque harmonic in ideal case. In this paper, it is not the research emphasis that how to decrease the fundamental cogging torque component 60th.

B. Cogging Torque for Stator Tolerances

No matter how high the precision of the stamping die, tolerance will always exist. The manufacturing tolerances on the stator can be summarized into the following three types:

1) tolerance of the stator tooth inner radius;
2) width tolerance of the stator tooth-shoe;
3) position tolerance of the stator tooth.

Actually all these tolerances can cause the slot opening tolerance. All manufacturing tolerances on the stator are shown in Fig. 6.

In Fig. 6, Δg is the decrement of the air gap because of the tolerance on the stator tooth inner radius; w_τ is the width of tooth-shoe; Δw_τ is the width tolerance of the tooth-shoe; $\Delta\beta_\tau$ is the position angle tolerance of the tooth.

When one of the stator teeth has a smaller inner radius as shown in Fig. 6 labeled with ①, (6) is rewritten to (10), shown below, and the coefficients can be calculated by (11) and (12).

$$\Lambda^2(\theta,\alpha) = \Lambda_0 + \sum_{n=1}^{\infty}\Lambda_n\cos\left(nz\left(\alpha+\theta\right)\right) + \Delta\Lambda_0 + \sum_{n=1}^{\infty}\Delta\Lambda_n\cos\left(n\left(\alpha+\theta\right)\right) \tag{10}$$

$$\Delta\Lambda_0 = \left(\left(\frac{1}{h_m+g-\Delta g}\right)^2 - \left(\frac{1}{h_m+g}\right)^2\right)\frac{\alpha_\tau}{z} \tag{11}$$

$$\Delta\Lambda_n = \frac{2z\Delta\Lambda_0}{n\pi\alpha_\tau}\sin\left(\frac{n\pi}{z}\alpha_\tau\right). \tag{12}$$

When one stator tooth-shoe is wider than the others as shown in Fig. 6 labeled with ②, the coefficients in (10) can be expressed as follows:

$$\Delta\Lambda_0 = \left(\frac{1}{h_m+g}\right)^2\frac{\Delta\alpha_\tau}{z} \tag{13}$$

$$\Delta\Lambda_n = \frac{2z\Delta\Lambda_0}{n\pi\Delta\alpha_\tau}\left(\sin\left(\frac{n\pi}{z}\left(\alpha_\tau+\Delta\alpha_\tau\right)\right) - \sin\left(\frac{n\pi}{z}\alpha_\tau\right)\right) \tag{14}$$

where $\Delta\alpha_\tau$ is the ratio of tooth-shoe width tolerances Δw_τ to slot pitch τ_s.

When one tooth is shifted from its normal position, one slot opening is wider and another one is smaller as shown in situation ③in Fig. 6, (6) and the coefficients can be, respectively, expressed as follows:

$$\Lambda^2(\theta,\alpha) = \Lambda_0 + \sum_{n=1}^{\infty}\Lambda_n\cos\left(nz\left(\alpha+\theta\right)\right) + \sum_{n=1}^{\infty}\Delta\Lambda_n\sin\left(n\left(\alpha+\theta+\frac{\pi}{360}\Delta\beta_t\right)\right) \tag{15}$$

$$\Delta\Lambda_n = -\frac{4}{n\pi}\left(\frac{1}{h_m+g}\right)^2\sin\left(\frac{n\pi\alpha_\tau}{z}\right)\sin\left(\frac{n\pi}{360z}\Delta\beta_t\right). \tag{16}$$

By comparing (10) and (15) with (6), it is easy to know that the additional components of the air gaps' relative permeance working with the air gaps' magnetic potential will yield additional cogging torque components, which can be expressed as follows:

$$\begin{aligned}\Delta T_{\mathrm{cog}}(\alpha) &= -\frac{L_{\mathrm{Fe}}}{4\mu_0}\left(R_2^2-R_1^2\right)\frac{\partial}{\partial\alpha}\int_0^{2\pi}\sum_{n=1}^{\infty}F_n\cos(2pn\theta)\\ &\quad\cdot\sum_{n=1}^{\infty}\Delta\Lambda_n\cos\left(n\left(\alpha+\theta\right)\right)d\theta\\ &= \frac{\pi L_{\mathrm{Fe}}}{4\mu_0}\left(R_2^2-R_1^2\right)\sum_{n=1}^{\infty}2pnF_n\Delta\Lambda_{2pn}\sin(2pn\alpha).\end{aligned} \tag{17}$$

Equation (17) shows that the frequencies of the additional components caused by stator tolerances are equivalent to a multiple of pole number $2p$. For the 10-pole/12-slot motors analyzed in this paper, stator tolerances cause 10th and 20th cogging torque components, which is the multiple of the pole number of 10.

C. Cogging Torque for Rotor Tolerances

Compared with those of the stator, tolerances of the rotor are not only from the lamination, but also from the PMs. The manufacturing tolerances on the rotor can also be summarized into the following six types:

1) tolerance of PM thickness;
2) tolerance of the rotor lamination outer radius;
3) width tolerance of the rotor magnet pole;
4) magnetization direction tolerance of PM;
5) position tolerance of the rotor PM;
6) tolerance of PMs' remanence.

These manufacturing tolerances on the rotor are shown in Fig. 7. In Fig. 7, Δh_m is the increment of the PM thickness; ΔR_1 is the increment of the rotor laminations' outer radius; w_p is the width of PM pole; Δw_p is the width tolerance of the PM pole; magnetization direction tolerance $\Delta\theta$ is the variation of the angle with respect to the magnetization direction; $\Delta\beta_m$ is the offset angle of the PM pole.

In the process of PM manufacture, cutting, and acid pickling may cause tolerances on the dimension of PMs. When the

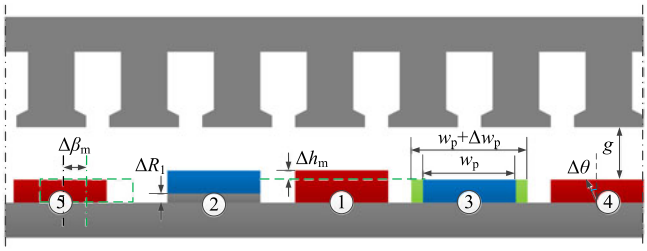

Fig. 7. Manufacturing tolerances on the rotor.

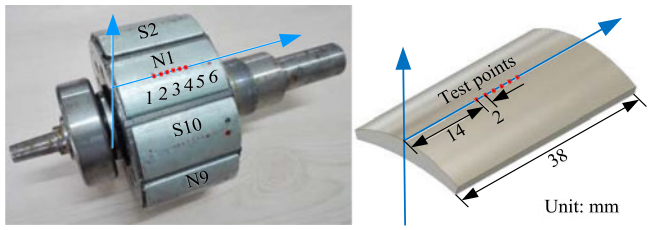

Fig. 8. Rotor and test points.

thickness of one PM pole is larger than that of the others, the magnetic potential will be influenced, and the corresponding expression of (5) is rewritten as (18), shown below, and the coefficients of each additional component are expressed as (19) and (20).

$$F^2(\theta) = F_0 + \sum_{n=1}^{\infty} F_n \cos(2pn\theta) + \Delta F_0 + \sum_{n=1}^{\infty} \Delta F_n \cos(n\theta) \tag{18}$$

$$\Delta F_0 = B_r^2 \left(\Delta h_m^2 + 2h_m \Delta h_m\right) \frac{\alpha_p}{2p} \tag{19}$$

$$\Delta F_n = \frac{4p\Delta F_0}{n\pi\alpha_p} \sin\left(n\pi \frac{\alpha_p}{2p}\right). \tag{20}$$

It is easy to understand that if the remanence of one PM is higher or the outer radius of the rotor lamination on a magnet position is larger, the same effect occurs with thicker magnets.

If the width of the PM is larger, the distribution of air gap flux is changed. Equations (21) and (22), shown below, can calculate the corresponding coefficients in (18)

$$\Delta F_0 = B_r^2 h_m^2 \frac{\Delta\alpha_p}{2p} \tag{21}$$

$$\Delta F_n = \frac{4p\Delta F_0}{n\pi\Delta\alpha_p} \left(\sin\left(\frac{n\pi}{2p}\left(\alpha_p + \Delta\alpha_p\right)\right) - \sin\left(n\pi\frac{\alpha_p}{2p}\right)\right) \tag{22}$$

where $\Delta\alpha_p$ is the ratio of pole width tolerances Δw_p to pole pitch τ_p.

If the PMs on the rotor surface are not evenly distributed, the air gap magnetic potential distribution along the rotor circumference will not be periodical. For example, if one PM has a position tolerance, (5) and corresponding coefficients can be expressed as follows:

$$F^2(\theta) = F_0 + \sum_{n=1}^{\infty} F_n \cos(2pn\theta) + \sum_{n=1}^{\infty} \Delta F_n \sin\left(n\left(\theta + \frac{\pi}{360}\Delta\beta_m\right)\right) \tag{23}$$

$$\Delta F_n = -\frac{4}{n\pi} B_r^2 h_m^2 \sin\left(\frac{n\pi\alpha_p}{2p}\right) \sin\left(\frac{n\pi}{720p}\Delta\beta_m\right). \tag{24}$$

Then, the additional cogging torque caused by these six tolerances is expressed as (25), shown below. These tolerances cause additional cogging torque components whose frequencies are equivalent to a multiple of stator slot number z. For the analyzed motors having 12-slots in this paper, rotor tolerances cause high amplitude of 12th cogging torque component, which is the multiple of the slot number of 12.

$$\begin{aligned}\Delta T_{\mathrm{cog}}(\alpha) &= -\frac{L_{\mathrm{Fe}}}{4\mu_0}\left(R_2^2 - R_1^2\right)\frac{\partial}{\partial\alpha}\int_0^{2\pi}\sum_{n=1}^{\infty}\Delta F_n\cos(n\theta) \\ &\quad\cdot\sum_{n=1}^{\infty}\Lambda_n\cos\left(nz\left(\alpha+\theta\right)\right)d\theta \\ &= \frac{\pi L_{\mathrm{Fe}}}{4\mu_0}\left(R_2^2 - R_1^2\right)\sum_{n=1}^{\infty} nz\Delta F_{nz}\Lambda_n\sin(nz\alpha).\end{aligned} \tag{25}$$

IV. Finite Element Analysis

A. Tolerances Assessment

The tolerances of stator and rotor laminations come from stamping die. By using a standard bore gage, the inner diameter tolerances of stator stacks are tested and they are about ± 0.035 mm. Hence, this value is used for dimensional tolerances of laminations.

In this paper, sintered NdFeB PMs with arc shape as shown in Fig. 8 are used. During the manufacturing of these PMs, machining and acid pickling are necessary and will cause dimensional error. According to the measurement, the thickness error of PMs used in the prototypes is about ± 0.05 mm. It is possible to decrease this tolerance. However, the cost will increase dramatically. Hence, ± 0.05 mm is used for dimensional tolerances of PMs.

The tolerance of PM remanence is mainly caused by nonuniform magnetization and this tolerance is approximately within $\pm 2\%$ with respect to the nominal remanence and the tolerance value of magnetization direction is within 1° sourced from manufacturer.

The dimensional error of the PMs is easy to measure. However, the remanence and magnetization direction tolerances are difficult to measure directly. To evaluate the remanence tolerance of PMs, the surface flux densities of all the poles are measured by using a Tesla meter and they are measured under open circuit state as shown in Fig. 8.

For each PM pole, six points are tested to decrease test error. The test points are evenly distributed and their positions on each PM are indicated in Fig. 8. The distance between each two test points is 2 mm. They are located at the symmetrical line of the PM. Fig. 9 compares the magnetic performance unifor-

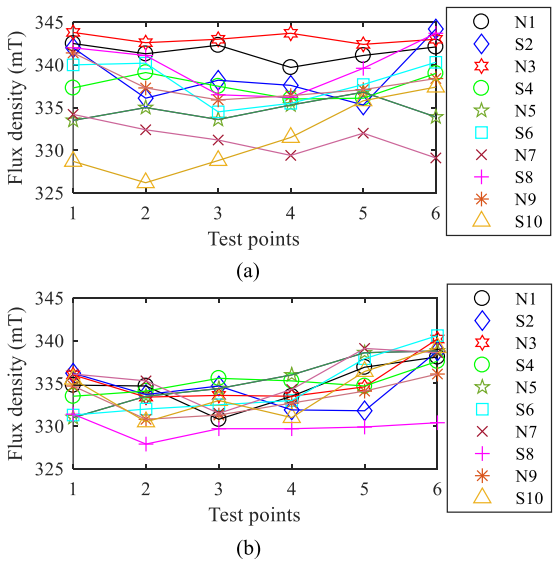

Fig. 9. Experimental results of surface flux densities. (a) Original rotor. (b) Even-PM rotor.

TABLE I
TOLERANCES OF PROTOTYPES

Item	Value
Stator inner diameter	±4.38%
Stator tooth-shoe width	±4.38%
Stator tooth position	4.38%
Rotor outer diameter	±4.38%
PM pole width	±6.25%
PM thickness	±6.25%
PM position	6.25%
PM remanence	±2%
PM magnetization direction	1°

mity of PM poles on the two rotors. In Fig. 9, each curve is corresponding to one PM pole. Fig. 9(a) is the test result of the original rotor and Fig. 9(b) is a better rotor with even magnets, which means the performance of all the ten PMs on the rotor are more uniform and this rotor is named even-PM rotor in this paper. Fig. 9(a) shows that the magnetic performance of the ten magnets on the original rotor is much different. The error of average surface flux densities of PMs on the original rotor is ±1.73%, which is close to the aforementioned ±2% from the manufacturer. Hence, in the paper ±2% is used for the remanence tolerance. The even-PM rotor has consistent magnets and their difference on average surface flux densities is equal to ±0.90%. As the tolerance with even-PM is relatively small, it is used for the experimental validation of stator tolerance influence in Section V.

Based on the measurement results and sources from manufacturers, the tolerances of the prototypes are summarized in Table I. The values of the dimensional and positional tolerances are expressed in percentage with respect to the air gap length, which is equal to 0.8 mm of the prototypes. In Table I, positive tolerance means the real value is larger than nominal value and vice versa. For example, negative tolerance of stator tooth radius will decrease the air gap length, whereas positive tolerance of stator tooth radius causes air gap length increasing.

B. Effects of Stator Tolerances

In order to determine which tolerance plays dominant role in the analyzed motor, the dimensional and positional tolerances of laminations and PMs have the same value. In this paper, the value ±6.25% is used. For instance, in Table II one tooth has 6.25% smaller radius, or one tooth-shoe is 6.25% wider than the nominal values, or one tooth is shifted away from its nominal position and this distance is 6.25% of the air gap length.

By using the FEA method, the influences of stator tolerances are analyzed and compared in Table II, which shows that the stator tolerances cause 10th and 20th components that are equivalent to a multiple of pole number $2p$, as illustrated by the analytical results. Furthermore, by comparing the amplitude of 10th component caused by stator tolerances in a normal error range, it is believed that the stator tooth inner radius has the highest impact on the cogging torque, whereas the other two tolerances have a smaller influence.

C. Effects of Rotor Tolerances

For PMs, the remanence tolerance is within ±2%. If one PM has 2% higher and another one has 2% lower remanence, the difference is 4%. Hence, 4% is used for the remanence tolerance. Since the magnetization direction tolerance sourced from manufacturer is equal to 1°, this value is used in FEA. The FEA results are shown in Table III.

The FEA results are very well in accordance with the analytical results: FEA results show that rotor tolerances cause 12th component that is equivalent to a multiple of slot number z. Furthermore, it can be seen that the remanence tolerance has the highest influence on the cogging torque; the thickness tolerance of the PM has the second highest impact; and the next is the outer radius tolerance of the rotor lamination. Compared with these three tolerances, the width, position, and magnetization direction tolerances of PMs have small influence on the cogging torque.

It can be noted that in Fig. 5, the four prototypes with larger stack length has different amplitudes, which can be explained as below. The 10th and 20th components are mainly generated by stator tolerances, which are decided by the stamping die. The stator tolerances of all the prototypes are almost the same since they are stamped from the same stamping die. Hence, the amplitude of these components of each prototype is similar. However, unlike in the case of the stator, the tolerances in the rotor mainly depend on the PMs, and each PM pole has different tolerance values. Because in this paper sintered PMs are used, they need machining to gain a specific form and this leads to dimension error. If bonded PMs from the same mould are used, the dimension error can be neglected. Besides, nonuniform magnetization causes magnetic performance difference. As a result, for each rotor, the total tolerance level is different. Consequently, the 12th components caused by rotor tolerance are much different in the four prototypes.

TABLE II
EFFECTS OF STATOR TOLERANCES

Stator tolerances	Stator tooth inner radius	Stator tooth-shoe width	Stator tooth position
Value	-6.25%	+6.25%	6.25%
FEA cogging torque	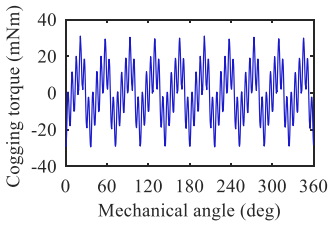	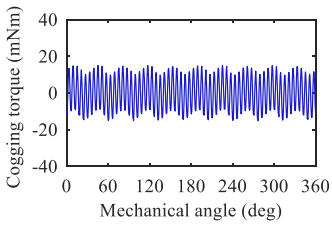	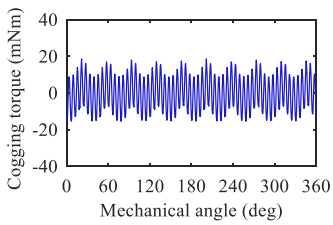
Amplitudes of cogging torque components	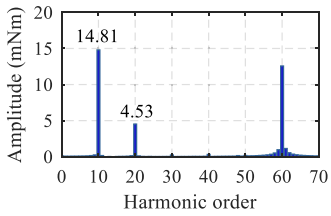	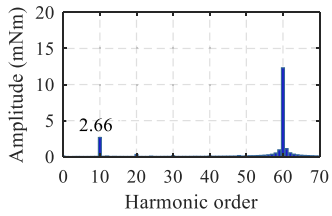	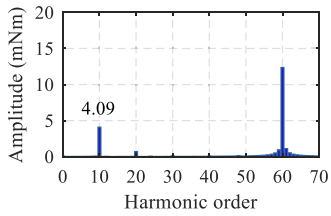
Importance	High	Low	Medium

TABLE III
EFFECTS OF ROTOR TOLERANCES

Rotor tolerances	PM thickness	Rotor stack outer radius	PM remanence
Value	+6.25%	+6.25%	+4%
FEA cogging torque	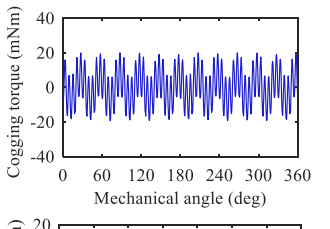	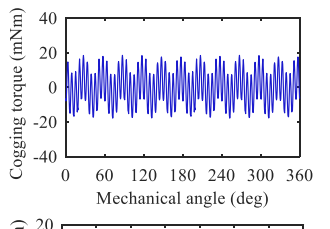	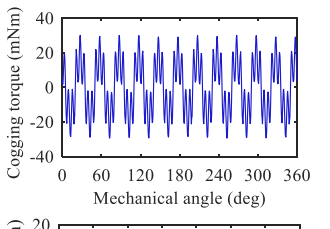
Amplitudes of cogging torque components	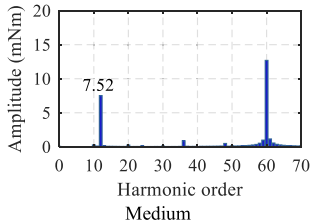	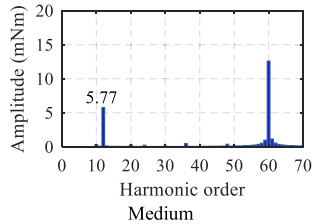	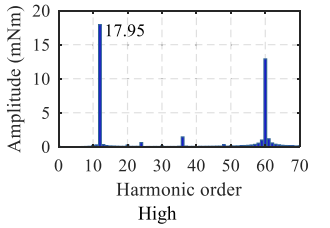
Importance	Medium	Medium	High

Rotor tolerances	PM width	PM position	PM magnetization direction
Value	+62.5%*	6.25%	1°
FEA cogging torque	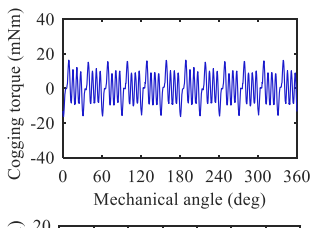	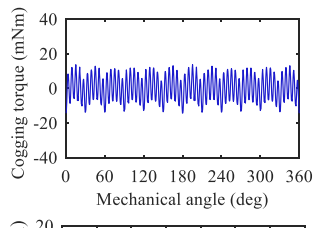	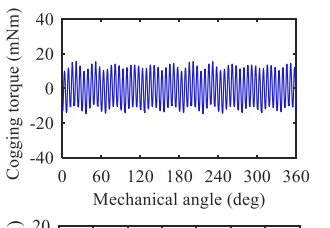
Amplitudes of cogging torque components	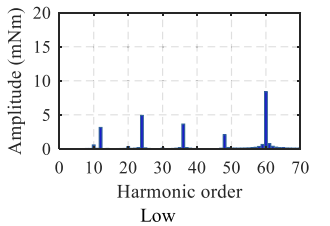	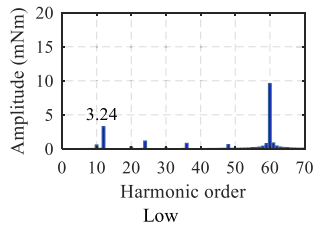	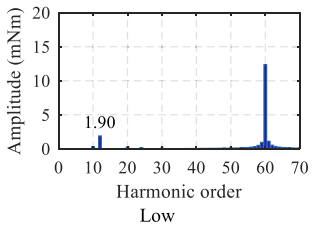
Importance	Low	Low	Low

* If one PM is 6.25% wider than the others, the amplitude of 12th cogging torque component is equal to 0.39 mNm. Thus, the importance of this tolerance is low. In order to show the components' orders caused by this tolerance clearly, the results shown in the TABLE III are corresponding to +62.5% wider PM.

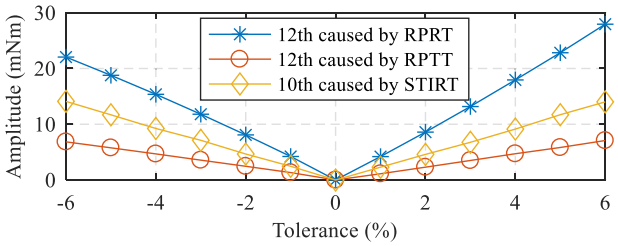

Fig. 10. Sensitivities of key tolerances on amplitude of cogging torque.

It can be concluded that the key tolerances in prototypes are stator inner radius and PM remanence tolerances. By integrating these key tolerances instead of all the tolerances into an optimization method, for instance, Taguchi's robust design method, in the design phase, a low cogging torque motor design can be obtained.

D. Sensitivities of Key Tolerances

It is known that in the prototypes, rotor PM remanence tolerance (RPRT) plays the most important role in causing low frequency cogging torque components, the second is the stator tooth inner radius tolerance (STIRT), followed by the rotor PM thickness tolerance (RPTT). RPRT and RPTT lead to cogging torque component of 12th, and STIRT results in 10th component. In Fig. 10, the sensitivities of these three tolerances are illustrated.

The FEA results show that the amplitudes of cogging torque components increase linearly when the absolute value of the tolerance increases. The signs of tolerances do not affect the orders of cogging torque components but have a small influence on amplitudes. Since the dimensional tolerances, STIRT and RPTT compared with the air gap length, is very low, the effect of signs is neglectable. However, as to the case of RPRT, positive tolerance generates higher amplitude compared with negative tolerance.

V. Experiment Verification and Improvement

A. Rotation Lamination Method

As the tolerances on the stator and rotor laminations come from the same stamping die, these tolerances are constant. If these tolerances are evenly distributed along the rotation circumference, the impact can be canceled out. Following this idea, a method named rotation lamination is proposed. When a new lamination is stamped, as shown in Fig. 11, before being laminated to the stack, the lamination stack needs to rotate along a fixed direction and the shift angle is equal to $360/z$ for the stator stack and $360/2p$ for the rotor stack. For example, since the slot number of the prototypes is 12, the shift angle of the stator stack is equal to 30°. To illustrate the rotation lamination method clearly, a gap is drawn on the edge of the lamination as shown in Fig. 11. It can be seen that the gaps of the laminations are evenly distributed on the stator stack after using the proposed method. Through the rotation lamination method, the errors of stator and rotor laminations are evenly distributed on the circumference. For the stacks produced by this method, they can be considered as error-free. Of course, this method will decrease the stamping efficiency.

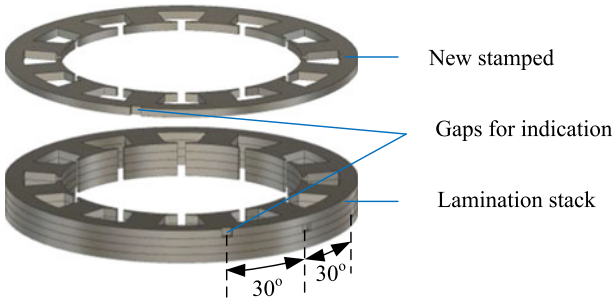

Fig. 11. Rotation lamination method.

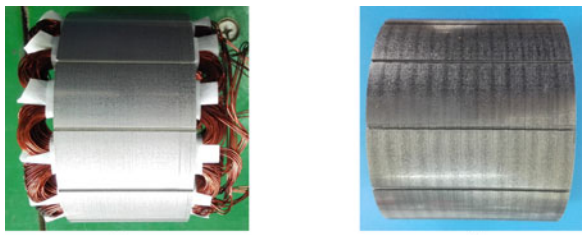

Fig. 12. Stator stacks. (a). Original. (b). Improved.

TABLE IV
Remanence Tolerances of Rotor Magnets

PM	N1	N3	S6	S8
Unit: %	4	3	5	3

After using the proposed method, the stator stack is shown in Fig. 12(b). By comparing the original stator stack without using the proposed method as shown in Fig. 12(a) with the improved stator stack, it can be noted that periodical traces occur on the surface of the improved stator stack. This means that the tolerances on the stator stack before improvement are significant. This method is also used to produce the rotor stack.

B. Rotor Tolerances Verification

When the improved stator with original rotor are used, that is, the tolerances of stator are suppressed by using the proposed method, the cogging torque only contains components with orders of slot number multiples such as 12th, 24th, and 36th. Since all rotor tolerances lead to cogging torque components of slot number multiples, and PM remanence tolerance is the main factor among them, in the FEA model, the equivalent PM remanence tolerances are used to take all the rotor tolerances into consideration. Therefore, the tolerances of the PMs for the FEA model in Table IV are higher than these in Table I. In Table IV, N1, N3, S6, and S8 are the magnets, which have remanence tolerances, and their positions in the rotor are shown in Fig. 1.

Fig. 13 is the FEA and test results of the prototype with improved stator and original rotor. It shows that after employing the proposed method to the stator, the cogging torques of 10th

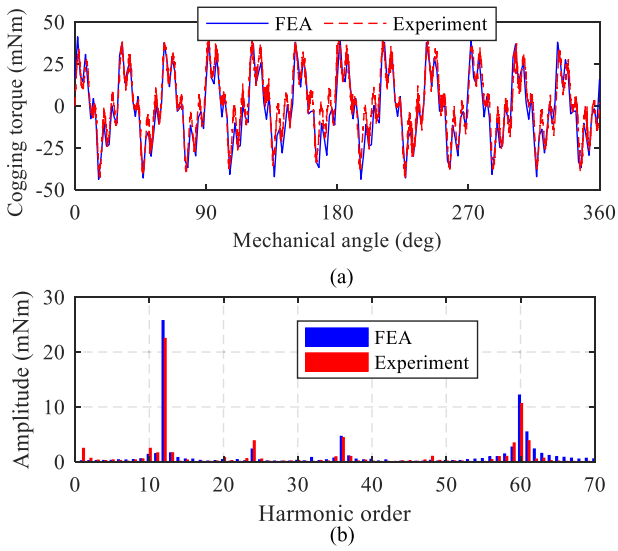

Fig. 13. FEA and experiment comparison of prototype with improved stator and original rotor.

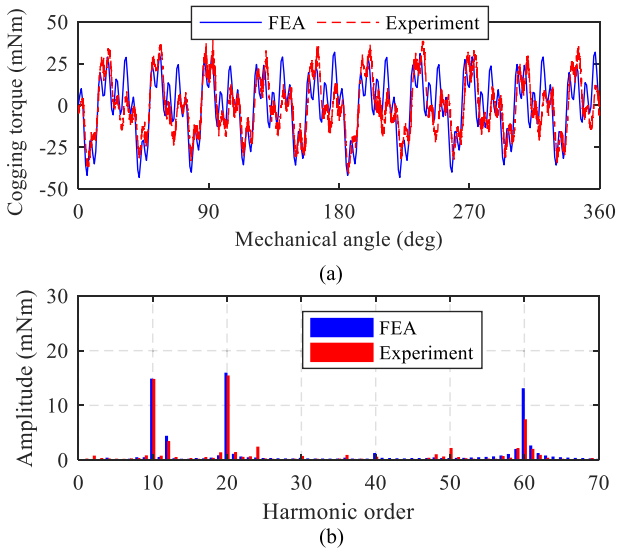

Fig. 14. FEA and experiment comparison of prototype with original stator and even-PM rotor.

and 20th caused by stator tolerances, are dramatically decreased, compared to that in Fig. 4, and only high 12th component due to rotor tolerance exists.

C. Stator Tolerances Verification

To eliminate the influence from the rotor tolerance, the even-PM rotor with original stator is tested, and the experimental results are shown in Fig. 14. According to the test results as shown in Fig. 9(b), the even-PM rotor has a small tolerance. Hence, one PM has 1% higher remanence is used in the FEA model. The equivalent tolerances of the stator inner radii are listed in Table V to represent all the stator tolerances, hence, the value in Table V is higher than that in Table I.

Due to the stator's tolerances, the cogging torque consists of high 10th and 20th components. Moreover, since the surface flux density on each pole still has a small difference, the 12th and 24th components are not totally suppressed.

From Sections V-B and C, it can be seen that the rotation lamination method to suppress the influence of stator tolerances is very effective, whereas the influence of rotor tolerances is unavoidable due to the PMs remanence tolerance. Therefore, in the design phase, more attention needs to be paid to the rotor tolerance to achieve a robust motor that is low sensitive to cogging torque.

TABLE V
TOLERANCES OF STATOR INNER RADII

Tooth	T3	T4	T6	T9	T10	T12
Unit: %	−6.25	−3.13	−6.25	−6.25	−3.13	−6.25

TABLE VI
TOLERANCES OF STATOR INNER RADII

Tooth	T3	T4	T6	T9	T10	T12
Unit: %	−6.88	−5.63	−5.63	−6.88	−5.63	−5.63

D. Stator and Rotor Tolerances Combination Verification

Since the tolerances in the motor are very difficult to measure, it is impossible to build an exactly same FEA model as the prototype. However, it is possible to build a consistent FEA model based on the analyses in Section IV. According to the former analysis and FEA verification, it is already known that the tolerance of stator inner radii is the main factor to cause multiples of the pole number components in cogging torque, whereas the PM remanence error is the key factor to cause multiples of the slot number components. From Figs. 4 and 5 it can be seen that in the original prototypes, the low frequency cogging torque components are with the order of 10th, 12th, and 20th. Hence, the equivalent tolerances of the stator inner radii and PM remanence error are considered to build the consistent FEA model.

The tolerances of stator inner radii are equal to those shown in Table VI, and the remanence of one PM is 4% higher than that of the others in the FEA model. The results of the FEA and experiment are compared in Fig. 15. From the two curves in Fig. 15(a), it can be seen that they are very close to each other. Fig. 15(b) also shows that the 10th, 12th, and 20th components of FEA and experiment have similar amplitudes. The comparison results not only verify the analyses before, but also clarify the causes of the low frequency cogging torque components in these prototypes, especially the values of these tolerances can be estimated. With the help of the results, solutions to decrease the cogging torque can be found.

E. Improvement on Prototypes

To evaluate the improvement after using the rotation lamination method, four prototypes named M1–M4 are tested and

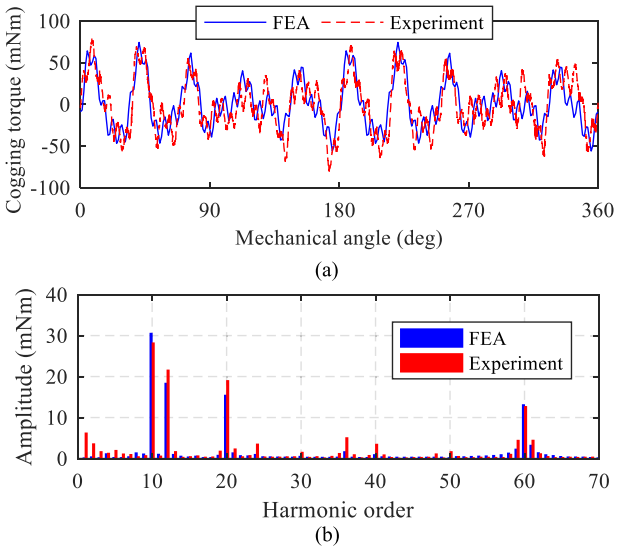

Fig. 15. FEA and experiment comparison of original prototype.

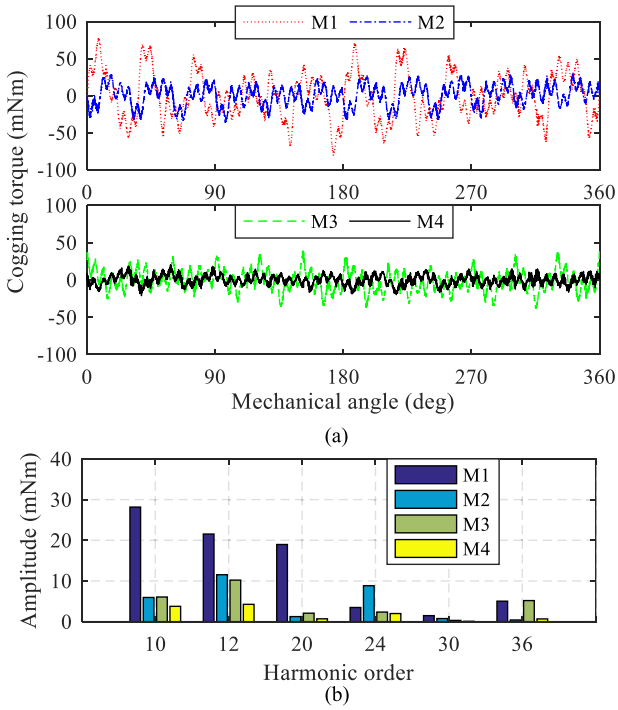

Fig. 16. Experimental results of original and improved prototypes.

the results are compared in Fig. 16 and Table VII. The four prototypes are as follows.

1) M1: prototype with original stator and rotor;
2) M2: proposed method used to build improved stator and rotor stacks, but the tolerances level of PMs is the same with original rotor;
3) M3: not only the improved stator and rotor stacks are used, but the PMs are also classified according to their thickness tolerances and this tolerance is within $\pm 1.88\%$;
4) M4: improved stator combines with even-PM rotor.

The peak values of these prototypes are listed in Table VII. By comparing M1 with M2, it can be noted that after improving stator and rotor stacks, the peak value of the cogging torque and the amplitudes of low-frequency components are decreased. This decrease is about 50%. By comparing M2 with M3, it is believed that classifying PMs according to their thickness tolerances cannot obviously improve the cogging torque performance. Although the 12th and 24th components caused by rotor tolerances are decreased after decreasing the thickness tolerance of PMs, the peak values of cogging torque of M2 and M3 are very close. This result is not difficult to understand. According to former analyses in Section IV, it is not PM thickness tolerance but the PM remanence tolerance play dominant role on causing low frequency cogging torque components. Hence, when even-PMs rotor are used, the cogging torque can be dramatically reduced as M4 does. Based on this solution, it is known that the PMs need to be classified according to their surface flux densities in order to decrease cogging torque caused by PMs' tolerances.

TABLE VII
PEAK VALUES OF ORIGINAL AND IMPROVED PROTOTYPES

Prototype	Maximum mN·m	Minimum mN·m
Original (M1)	79.0	−80.4
Improved stacks (M2)	40.5	−40.7
Improved stacks with small dimension error PMs (M3)	41.5	−38.7
Improved stator stack with even-PM rotor (M4)	20.3	−21.2

These experimental results not only verify the theoretical and FEA analyses but confirm the effectiveness of the proposed manufacturing methods as well. To decrease the sensitivity of tolerances, the two key tolerances, stator tooth inner radius and PM remanence, need to be considered at the phase of motor design.

VI. CONCLUSION

The cogging torque caused by manufacturing tolerances was analyzed systematically and comprehensively. Based on energy variations method, the low-frequency components caused by stator and rotor tolerances were separated. Through FEA and experiments, it was validated that the stator tolerances cause cogging torque components that are equivalent to a multiple of the rotor pole number $2p$, whereas rotor tolerances cause components equivalent to a multiple of the stator slot number z. The inner radius tolerance of the stator has the largest influence on cogging torque among the stator tolerances, whereas the remanence of PMs is the main contributor to rotor tolerances. This is followed by the PM thickness and the rotor outer radius tolerances. By combining the energy variations and FEA, the causes of the low-frequency cogging torque components in a prototype can be elaborated. Hence, solutions to decrease the cogging torque can be found. Moreover, it also provides the designers with a guidance to set the limits of tolerances in the design phase for manufacturing process to produce motors with low cogging torque. To achieve the target on cogging torque

for massive production, in the design phase, the key tolerances must be determined. Special design and optimization must be done to consider these tolerances to decrease the sensitivity of them. In addition, the maximum allowable tolerances need to be estimated in the worst case. When all the stator tolerances occur on one tooth and all the rotor tolerances happen on one pole, the cogging torque reaches its highest value. Then, these tolerances' values can be later used as a criterion for manufacturers of PMs and stamping die. By this way, it is more effective for the design and massive production of motors with low cogging torque.

To reduce the influence of the stator and rotor stacks' tolerance, a manufacturing method for producing stator and rotor stacks was proposed and used to build the improved stator and rotor stacks. To mitigate the influence of the PM tolerances, it was suggested to classify PMs according to their surface flux densities. By combining the two methods, the cogging torque of the motor is reduced by about 75%. However, classifying PMs according to their magnetic performance is time-consuming and increases the manufacture cost. When only the improved stator and rotor stacks are used, the cogging torque can still be reduced by about 50%. This improvement is remarkable as the precision of the stamping model can be lowered to decrease the manufacturing cost without affecting cogging torque. Of course, the efficiency of the stamping may be decreased because of the rotation requirement. Future research will be toward integrating the PMs' remanence into the design process of the motor in order to decrease their impacts on cogging torque.

Acknowledgment

The authors would like to thank Prof. B. Song and L. Wu from Huazhong University of Science and Technology and H. Bi, G. Yang, and C. Du from Wuhan Numerical Control Corporation for their help with experiments and prototypes' design.

References

[1] L. J. Wu, Z. Q. Zhu, D. A. Staton, M. Popescu, and D. Hawkins, "Comparison of analytical models of cogging torque in surface-mounted PM machines," *IEEE Trans. Ind. Electron.*, vol. 59, no. 6, pp. 2414–2425, Jun. 2012.

[2] Y. Zhou, H. Li, G. Meng, S. Zhou, and Q. Cao, "Analytical calculation of magnetic field and cogging torque in surface-mounted permanent-magnet machines accounting for any eccentric rotor shape," *IEEE Trans. Ind. Electron.*, vol. 62, no. 6, pp. 3438–3447, Jun. 2015.

[3] A. J. Piña Ortega, S. Paul, R. Islam, and L. Xu, "Analytical model for predicting effects of manufacturing variations on cogging torque in surface-mounted permanent magnet motors," *IEEE Trans. Ind. Appl.*, vol. 52, no. 4, pp. 3050–3061, Jul./Aug. 2016.

[4] J. Wanjiku, M. A. Khan, P. S. Barendse, and P. Pillay, "Influence of slot openings and tooth profile on cogging torque in axial-flux PM machines," *IEEE Trans. Ind. Electron.*, vol. 62, no. 12, pp. 7578–7589, Dec. 2015.

[5] D. Wang, X. Wang, M. K. Kim, and S. Y. Jung, "Integrated optimization of two design techniques for cogging torque reduction combined with analytical method by a simple gradient descent method," *IEEE Trans. Magn.*, vol. 48, no. 8, pp. 2265–2276, Aug. 2012.

[6] Y. Li, Q. Lu, Z. Q. Zhu, D. Wu, and G. Li, "Superposition method for cogging torque prediction in permanent magnet machines with rotor eccentricity," *IEEE Trans. Magn.*, vol. 52, no. 6, pp. 1–10, Jun. 2016.

[7] S. A. Saied, K. Abbaszadeh, A. Tenconi, and S. Vaschetto, "New approach to cogging torque simulation using numerical functions," *IEEE Trans. Ind. Appl.*, vol. 50, no. 4, pp. 2420–2426, Jul./Aug. 2014.

[8] D. Wang, X. Wang, and S. Y. Jung, "Cogging torque minimization and torque ripple suppression in surface-mounted permanent magnet synchronous machines using different magnet widths," *IEEE Trans. Magn.*, vol. 49, no. 5, pp. 2295–2298, May 2013.

[9] C. Xia, Z. Chen, T. Shi, and H. Wang, "Cogging torque modeling and analyzing for surface-mounted permanent magnet machines with auxiliary slots," *IEEE Trans. Magn.*, vol. 49, no. 9, pp. 5112–5123, Sep. 2013.

[10] T. Liu, S. Huang, J. Gao, and K. Lu, "Cogging torque reduction by slot-opening shift for permanent magnet machines," *IEEE Trans. Magn.*, vol. 49, no. 7, pp. 4028–4031, Jul. 2013.

[11] Y. Li, Q. Lu, Z. Q. Zhu, D. Wu, and G. Li, "Superposition method for cogging torque prediction in permanent magnet machines with rotor eccentricity," *IEEE Trans. Magn.*, vol. 52, no. 6, pp. 1–10, Jun. 2016.

[12] Z. Q. Zhu, L. J. Wu, and M. L. Mohd Jamil, "Influence of pole and slot number combinations on cogging torque in permanent-magnet machines with static and rotating eccentricities," *IEEE Trans. Ind. Appl.*, vol. 50, no. 5, pp. 3265–3277, Sep. /Oct. 2014.

[13] P. Jalali, S. Taghipour Boroujeni, and N. Bianchi, "Analytical modeling of slotless eccentric surface-mounted PM machines using a conformal transformation," *IEEE Trans. Energy Convers.*, vol. 32, no. 2, pp. 658–666, Jun. 2017.

[14] J. Fu and C. Zhu, "Subdomain model for predicting magnetic field in slotted surface mounted permanent-magnet machines with rotor eccentricity," *IEEE Trans. Magn.*, vol. 48, no. 5, pp. 1906–1917, May 2012.

[15] J. M. Kim, M. H. Yoon, J. P. Hong, and S. I. Kim, "Analysis of cogging torque caused by manufacturing tolerances of surface-mounted permanent magnet synchronous motor for electric power steering," *IET Elect. Power Appl.*, vol. 10, no. 8, pp. 691–696, Sep. 2016.

[16] H. Qian, H. Guo, Z. Wu, and X. Ding, "Analytical solution for cogging torque in surface-mounted permanent-magnet motors with magnet imperfections and rotor eccentricity," *IEEE Trans. Magn.*, vol. 50, no. 8, pp. 1–15, Aug. 2014.

[17] Z. Q. Zhu, Z. Azar, and G. Ombach, "Influence of additional air gaps between stator segments on cogging torque of permanent-magnet machines having modular stators," *IEEE Trans. Magn.*, vol. 48, no. 6, pp. 2049–2055, Jun. 2012.

[18] X. Ge and Z. Q. Zhu, "Influence of manufacturing tolerances on cogging torque in interior permanent magnet machines with eccentric and sinusoidal rotor contours," *IEEE Trans. Ind. Appl.*, vol. 53, no. 4, pp. 3568–3578 , Jul./Aug. 2017.

[19] I. Coenen, M. van der Giet, and K. Hameyer, "Manufacturing tolerances: Estimation and prediction of cogging torque influenced by magnetization faults," *IEEE Trans. Magn.*, vol. 48, no. 5, pp. 1932–1936, May 2012.

[20] S.-M. Hwang, J. -B. Eom, Y. -H. Jung, D.-W. Lee, and B. -S. Kang, "Various design techniques to reduce cogging torque by controlling energy variation in permanent magnet motors," *IEEE Trans. Magn.*, vol. 37, no. 4, pp. 2806–2809, Jul. 2001.

[21] M. Markovic, M. Jufer, and Y. Perriard, "Reducing the cogging torque in brushless DC motors by using conformal mappings," *IEEE Trans. Magn.*, vol. 40, no. 2, pp. 451–455, Mar. 2004.

[22] L. Gu, E. Bostanci, M. Moallem, S. Wang, and P. Devendra, "Analytical calculation of the electromagnetic field in SRM using conformal mapping method," in *Proc. IEEE Transp. Electrific. Conf. Expo.*, Dearborn, MI, 2016, pp. 1–6.

[23] L. Zhu, S. Z. Jiang, Z. Q. Zhu, and C. C. Chan, "Analytical methods for minimizing cogging torque in permanent-magnet machines," *IEEE Trans. Magn.*, vol. 45, no. 4, pp. 2023–2031, Apr. 2009.

[24] L. Zhu, S. Z. Jiang, Z. Q. Zhu, and C. C. Chan, "Comparison of alternate analytical models for predicting cogging torque in surface-mounted permanent magnet machines," in *Proc. IEEE Veh. Power Propulsion Conf.*, Harbin, 2008, pp. 1–6.

Jing Ou (S'16) was born in Guangdong, China. He received the B.E.E. and M.S.E.E. degrees in electrical engineering from Harbin Institute of Technology, Harbin, China, in 2011 and 2013, respectively. He has been working toward the Ph.D. degree in electrical engineering and information technologies from Karlsruhe Institute of Technology, Karlsruhe, Germany, since 2015.

His research interests include the design and control of electrical machines.

Yingzhen Liu (S'13) was born in Hebei, China. She received the B.E.E. degree from Harbin Institute of Technology, Harbin, China, in 2011 and the M.S.E.E. degree from Huazhong University of Science and Technology, Wuhan, China, in 2014, both in electrical engineering. She is currently working toward the Ph.D. degree in electrical engineering and information technologies from Karlsruhe Institute of Technology, Karlsruhe, Germany.

Her research interest is machine design, especially the design of superconducting wind generators.

Ronghai Qu (S'01–M'02–SM'05) was born in China. He received the B.E.E. and M.S.E.E. degrees from Tsinghua University, Beijing, China, in 1993 and 1996, respectively, and the Ph.D. degree from the University of Wisconsin-Madison, Madison, WI, USA, in 2002, all in electrical engineering.

In 1998, he joined the Wisconsin Electric Machines and Power Electronics Consortiums as a Research Assistant. He became a Senior Electrical Engineer with Northland, a Scott Fetzer Company, in 2002. Since 2003, he has been with the General Electric (GE) Global Research Center, Niskayuna, NY, USA, as a Senior Electrical Engineer with the Electrical Machines and Drives Laboratory. He has authored more than 120 published technical papers and is the holder of more than 50 patents/patent applications. Since 2010, he has been a Professor with Huazhong University of Science and Technology, Wuhan, China.

Prof. Qu is a full member of Sigma Xi. He has received several awards from GE Global Research Center since 2003, including the Technical Achievement and Management Awards. He also received the 2003 and 2005 Best Paper Awards, third prize, from the Electric Machines Committee of the IEEE Industry Applications Society at the 2002 and 2004 IAS Annual Meetings, respectively.

Martin Doppelbauer was born in Altenhundem, Germany. He received the Dipl.Ing. and Dr. Ing. degrees in electrical engineering from the University of Dortmund, Dortmund, Germany, in 1990 and 1995, respectively.

He was with Danfoss Bauer, Esslingen, Germany, and SEW Eurodrive, Bruchsal, Germany, as a Senior Manager for electric motor development. He has held the professorship for hybrid electric vehicles at Karlsruhe Institute of Technology, Karlsruhe, Germany, since 2011.